

National Transportation Library

Section 508 and Accessibility Compliance

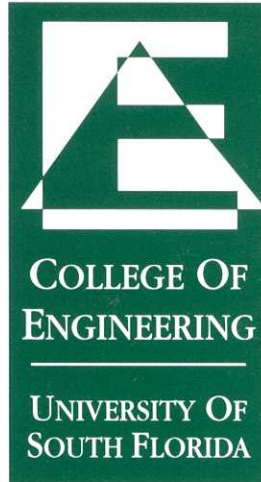
The National Transportation Library (NTL) both links to and collects electronic documents in a variety of formats from a variety of sources. The NTL makes every effort to ensure that the documents it collects are accessible to all persons in accordance with Section 508 of the Rehabilitation Act Amendments of 1998 (29 USC 794d), however, the NTL, as a library and digital repository, collects documents it does not create, and is not responsible for the content or form of documents created by third parties. Since June 21, 2001, all electronic documents developed, procured, maintained or used by the federal government are required to comply with the requirements of Section 508.

If you encounter problems when accessing our collection, please let us know by writing to librarian@bts.gov or by contacting us at (800) 853-1351. Telephone assistance is available 9AM to 6:30PM Eastern Time, 5 days a week (except Federal holidays). We will attempt to provide the information you need or, if possible, to help you obtain the information in an alternate format. Additionally, the NTL staff can provide assistance by reading documents, facilitate access to specialists with further technical information, and when requested, submit the documents or parts of documents for further conversion.

Document Transcriptions

In an effort to preserve and provide access to older documents, the NTL has chosen to selectively transcribe printed documents into electronic format. This has been achieved by making an OCR (optical character recognition) scan of a printed copy. Transcriptions have been proofed and compared to the originals, but these are NOT exact copies of the official, final documents. Variations in fonts, line spacing, and other typographical elements will differ from the original. All transcribed documents are noted as "Not a True Copy."

The NTL Web site provides access to a graphical representation of certain documents. Thus, if you have any questions or comments regarding our transcription of a document's text, please contact the NTL at librarian@bts.gov. If you have any comment regarding the content of a document, please contact the author and/or the original publisher.



IMPLEMENTATION OF SHRP
CORROSION DIAGNOSIS PROJECTS IN PLANNING
MAINTENANCE STRATEGIES FOR FLORIDA BRIDGES
State Job 99700-3560-119, WPI 0510862
Contract No. BB-259
Final Report to Florida Department of Transportation

Alberto A. Sagüés
Principal Investigator
Department of Civil and Environmental Engineering

UNIVERSITY OF SOUTH FLORIDA ■ COLLEGE OF ENGINEERING
4202 EAST FOWLER AVENUE ■ ENB 118 ■ TAMPA, FLORIDA 33620-5350
PHONE: (813) 974-3780 ■ FAX: (813) 974-5094

WEB SITE: WWW.ENG.USF.EDU

Report Prepared by :

Alberto. A. Sagüés

**IMPLEMENTATION OF SHRP
CORROSION DIAGNOSIS PROJECTS IN PLANNING
MAINTENANCE STRATEGIES FOR FLORIDA BRIDGES**

State Job 99700-3560-119, WPI 0510862

Contract No. BB-259

Final Report to Florida Department of Transportation

**Alberto A. Sagüés
Principal Investigator
Department of Civil and Environmental Engineering**

**University of South Florida
Tampa, FL, 33620
March 31,2002**

1 Report No BB-259	2 Government Accession No <i>NIN /nev</i>	3 Recipient's Catalog No <i>TRIS AN 00925812</i>	
4 Title and Subtitle IMPLEMENTATION OF SHRP CORROSION DIAGNOSIS PROJECTS IN PLANNING MAINTENANCE STRATEGIES FOR FLORIDA BRIDGES		5 Report Date March 31, 2002	
		6 Performing Organization Code	
		8 Performing Organization Report No	
7 Author's Alberto. A. Sagüés		10 Work Unit No (TRAIS)	
9 Performing Organization Name and Address Department of Civil and Environmental Engineering University of South Florida Tampa, FL 33620		11 Contract or Grant No BB-259	
		13 Type of Report and Period Covered Final Report Aug. 1997-Sept. 2001	
12 Sponsoring Agency Name and Address Florida Department of Transportation 605 Suwannee Street Tallahassee, FL 32399-0450		14 Sponsoring Agency Code	
		15 Supplementary Notes Prepared in cooperation with the U.S. Department of Transportation and the Federal Highway Administration	
16 Abstract <p>The Strategic Highway Research Program (SHRP) was active between 1988 and 1993 with support from Federal and State sources including Florida. A large part of the SHRP effort was aimed at developing techniques for the assessment and prevention of corrosion deterioration in bridges exposed to deicing salt regimes, of limited relevance to the modes of deterioration encountered in Florida Department of Transportation (FDOT) structures, or formulated in a manner that requires the development of implementation for specific service environments. In this project the suitability of the main products developed under SHRP C-101 and C-103 was evaluated for application to FDOT needs. Work concentrated on using the methodology for corrosion forecasting developed under C-103 as a starting point for a procedure suitable for marine substructure. Development consisted in introducing variability in the parameters responsible for corrosion initiation and propagation, obtaining equations for calculating the overall damage function for a marine substructure. Examples of application of the procedure are cited for the Escambia Bay Bridges, and for the analysis of corrosion prognosis for major Florida Keys bridges built using epoxy coated rebar.</p>			
17 Key Words Reinforcing Steel, Corrosion, Chlorides, Concrete, SHRP, Durability, Forecast, Methodology		18 Distribution Statement No restrictions. This document is available to the public through the National Technical Information Service, Springfield, VA 22161	
19 Security Classif (of this report) Unclassified	20 Security Classif (of this page) Unclassified	21 No of Pages 43	22 Price

TABLE OF CONTENTS

1. EXECUTIVE SUMMARY	3
2. INTRODUCTION	4
3. EVALUATION OF APPLICABLE SHRP PRODUCTS	5
4. DAMAGE PROGRESSION MODEL	11
5. CASE APPLICATION - ESCAMBIA BAY BRIDGES	14
6. CASE APPLICATION - FLORIDA KEYS BRIDGES BUILT WITH EPOXY COATED REBAR	20
7. DISCUSSION OF CASE APPLICATIONS	26
8. CONCLUSIONS	27
9. REFERENCES	28
10. TABLES	33
11. FIGURES	36
12 UNITS CONVERSION TABLE	43

NOTICE

The opinions, findings and conclusions expressed in this publication are those of the authors and not necessarily those of the State of Florida Department of Transportation. Prepared in cooperation with the State of Florida Department of Transportation. The assistance in the field investigations of personnel of the Corrosion group at the FDOT Materials Office is gratefully acknowledged.

1. EXECUTIVE SUMMARY

The Strategic Highway Research Program (SHRP) was active between 1988 and 1993 with support from Federal and State sources including Florida. Much of the effort aimed at developing techniques for the assessment and prevention of corrosion deterioration of the nation's infrastructure, but focused on the problem of corrosion of reinforcement in bridges exposed to deicing salt regimes. That focus was of limited relevance to the corrosive marine environments encountered in FDOT structures. The objectives of this project were to identify the SHRP corrosion control product(s) with most potential to serve the needs of the FDOT, and to adapt that technology as appropriate. Emphasis was given to examining products from SHRP projects C-101 (assessment of corrosion deterioration) and C-103 (non-electrochemical repair and maintenance methods).

Of the C-101 SHRP products, that which addressed corrosion rate devices was found to hold promise of direct application to marine substructure corrosion assessment. One of the test devices appears to be reasonably suitable for implementation of the technology. The other C-101 products address primarily specialized bridge deck corrosion assessment situations. A procedure for estimating residual service life under the product from SHRP C-103, *Life Cycle Cost Analysis Methodology*, was found to merit further development and adaptation to FDOT needs, which was conducted as the main thrust of the present project.

Development starting from the C-103 procedure for estimating residual service life showed that quantitative projections of future deterioration and interpretation of historical damage development can be performed by taking into account the compounded variability of concrete cover, chloride diffusivity, and chloride surface concentration in the substructure of marine bridges. The procedure was applied and demonstrated for two cases of direct relevance to the FDOT service conditions: corrosion forecasting of the Escambia Bay Bridges, and assessment of corrosion modes and prognosis of major bridges in the Florida Keys built using epoxy coated rebar. The projected damage functions reflected the dispersion of the assumed controlling model variables. The model approach is not an absolute prediction tool, but should be viewed instead as a means to assist in comparing design alternatives.

The procedure developed under the present project is recommended for use in estimating corrosion-related damage progression in the substructure of marine bridges in the FDOT inventory. Areas for future improvement of this methodology include accounting for effective diffusivity and surface concentration variations with time, the effect of chloride ion binding on diffusion, the effect of rebar potential on corrosion threshold, and a more precise evaluation of the length of the corrosion propagation stage.

2. INTRODUCTION

The Strategic Highway Research Program (SHRP) was active between 1988 and 1993 with \$30 million support from Federal and State sources including Florida. A large part of the SHRP effort was aimed at developing techniques for the assessment and prevention of corrosion deterioration of the nation's infrastructure. Notable SHRP projects with this aim included Contracts C-101 for the assessment of corrosion deterioration, C-102 for electrochemical corrosion protection techniques (primarily cathodic protection), C-103 for non-electrochemical repair and maintenance methods, and the SHRP-IDEA initiative. The program created a vast amount of useful information and products [1] which are only now beginning to encounter significant application by individual states. Some of those products, such as the use of sprayed zinc sacrificial anodes developed jointly by FDOT and University of South Florida under SHRP-IDEA Project No. 24, have been of immediate use in the maintenance of FDOT bridges [2]. However, the bulk of the SHRP corrosion control effort has been either focused on the problem of corrosion of reinforcement in bridges exposed to deicing salt regimes (of limited relevance to the modes of deterioration encountered in FDOT structures [3-6]), or formulated in a manner that requires the development of implementation for specific service environments.

The Department has a bridge inventory of over 5,500 structures of which nearly two thirds are exposed to corrosive marine environments. While research projects are now underway to optimize design in new structures, condition evaluation of new structures and the development of adequate maintenance strategy is a continuing, immediate need. It was desirable to examine the evaluation techniques developed under SHRP for diagnosing the condition of FDOT structures and applying the results to develop an adequate corrosion damage forecasting strategy.

The objectives of this project were therefore :

- 1) to identify the SHRP corrosion control product(s) with most potential to serve the needs of the FDOT.
- 2) to transfer that technology to the cases of marine substructure deterioration in warm environments that reflect the corrosion-related maintenance needs in the State.

The outcome of this project consisted of:

- 1) a summary evaluation of diagnostic procedures.
- 2) a procedure for estimating residual service life and needs for future maintenance.
- 3) case applications of the forecasting procedure.

3. EVALUATION OF APPLICABLE SHRP PRODUCTS

SCOPE

Products addressing diagnostic and maintenance procedures were considered. The diagnostic procedures included most of those currently disseminated by FHWA Demonstration Project 84 and developed under SHRP C-101. Those procedures are detailed in the 8-volume SHRP-S-331 report "Condition Evaluation of Concrete Bridges Relative to Reinforcement Corrosion" [1] and include a variety of methods for the electrochemical determination of the corrosion state of steel, and assessment of the extent of penetration of chloride ions in the concrete. The present work involved both review of the available literature and execution of exploratory laboratory tests with the selected techniques and instrumentation, including equipment on loan from the FHWA Demonstration Project 84. The findings for that activity are presented only in summary form.

Application to maintenance procedures assessed the applicability to Florida service of SHRP documents such as SHRP-S-360 "Concrete Bridge Protection, Repair and Rehabilitation Relative to Reinforcement Corrosion: A Methods Application Manual" [7] and was facilitated by adapting, whenever appropriate, the methodologies developed under the recently completed FDOT project WPI 0510805 "Corrosion Forecasting for 75-Year Durability Design of Reinforced Concrete" [8] for the selection of design parameters and prediction of design service life in new structures. Of special interest was the application of chloride profiling to estimate the residual service time to corrosion in existing structures.

PRODUCTS CONSIDERED

Product 2001, *Corrosion Rate Devices*.

This Product created a standard test method to measure corrosion rates in existing structures by means of polarization resistance (R_p) measurements using devices that perform nearly direct current (DC) measurements of the polarization response of the reinforcing steel. The devices measure also the solution resistance (R_s) of the concrete for appropriate correction of the results.

Three devices were addressed by the SHRP method: 3LP, Gecor and PR-Monitor. Of those, both the Gecor and PR-Monitor devices use a guard-ring electrode to provide signal confinement and reduce uncertainty in the steel area being evaluated. Because in marine substructures concrete resistivity can be small and corrosion macrocell effects significant, signal confinement is a concern. Thus, only the Gecor and PR-Monitor devices were investigated. Test units of each type were obtained on loan from the inventory in FHWA Demonstration Project 84.

The devices were evaluated in the laboratory to establish the validity of corrosion rate values by comparing the corresponding polarization resistance values with those

obtained with electrochemical impedance spectroscopy (EIS) for a system that had been previously characterized in detail for its static and dynamic electrochemical behavior [3,9]. The system consisted of instrumented laboratory columns partially submerged in salt water, with multiple interconnected black rebar segments. A corrosion macrocell pattern developed in each column [9,10,12], with the cathodic reaction taking place predominantly in the rebar segments above water. EIS measurements were performed on individual segments, using an internal activated Titanium reference electrode, and all the other rebar segments of the column as a large counter electrode. A high-impedance current source was used to provide a.c. isolation between the segment tested and the other interconnected elements [10, 11].

The electrochemical parameters for oxygen reduction in the segments above water were accurately determined and a quantitative correlation between EIS response and the rate of the reactions on the steel surface was well established so that the behavior of the PR-Monitor and the Gecor device could be contrasted against the independently known behavior. The devices under those conditions report a fictitious corrosion rate (actually the rate of the cathodic reaction only) but that can be used to assess current confinement. All measurements were made for conditions corresponding to nearly passive steel in a freely corroding system, where the possibilities for misleading diagnosis would be greatest. The following is a summary of the findings:

1. The ratio of polarization resistance values (in $k\Omega/cm^2$) determined by EIS to those determined with the Gecor device (which uses a galvanostatic step of 100 s) was between 1 and 3. Thus, nominal corrosion rate values obtained with the Gecor device were in reasonable order of magnitude agreement with the expected values considering the uncertainty inherent in electrochemical corrosion rate determination of corrosion rates in concrete [13].
2. The ratio of polarization resistance values (in $k\Omega/cm^2$) determined by EIS to those determined with the PR-Monitor (which uses a potentiostatic technique) was between 5 to 15 for a scan rate of 0.05 mV/s. It appears that, due to the long polarization times needed to achieve steady-state, the values of i_{corr} measured with this device for a passive system could appreciably overestimate the actual values.
3. The reproducibility of the measurements made with these devices was assessed by performing 3 measurements within 5 to 10 min from each other, at each position in the column. The reproducibility for both devices, expressed as the estimated error in the mean ($\sigma n^{-1/2}$) was similar to that found by other authors [14] with the Gecor device under laboratory conditions.
5. Additional observations in the operation of the Gecor device are:
 - a) The message "current confinement not fully achieved" often appeared when measurements were made just above the water line.
 - b) The test assembly (probe "A") required periodic maintenance of the reference electrodes, to avoid introduction of air bubbles or drying.

c) There was little information in the manual on the degree of achievable current confinement.

6. With the PR-Monitor polarization could only be implemented toward potentials more noble than the corrosion potential, thus allowing risk of accidental excessive anodic excursions.

The findings summarized here suggest that this methodology can provide useful additional information on the corrosion state of a marine bridge substructure member. However, the value of that information is limited by possible measurement artifacts. Of the two devices tested, the Gecor device appeared to provide the most reliable overall indications.

As the devices considered (or next-generation units based on similar methodology) are commercially available, no further development was deemed necessary at this time.

Product 2030, *Field Chloride Content*.

This product was evaluated by consideration of the results available in the literature and of the needs for accuracy and reliability inherent for durability forecasting of marine substructure.

The SHRP methodology is aimed to speed of determination and minimization of sample extraction and analysis costs. The approach consists of extracting concrete powder samples by small-diameter (19 mm) drilling at different depths from the surface, and performing on-site chemical analysis for chloride content using a simple potentiometric technique. The quick sampling and analysis in the SHRP method is at the expense of analysis accuracy when compared with traditional coring and laboratory titrations. The technique may be advantageous for volume-intensive examinations of bridge decks and other easily accessible structural elements.

In a marine substructure environment accessibility to the structural elements to be analyzed is usually very limited, often as a result of weather, sea roughness and tides. Consequently much of the cost of obtaining a chloride concentration profile reflects crew idle time and water craft expenses in accessing the sampling location. For the same reason, the number of locations sampled in marine substructures tends to be relatively small. Once a location is accessed, conventional concrete coring for later laboratory analysis can be performed relatively rapidly, in about the same time as it would take to drill and collect powder samples at several depths. Under those conditions, precise chloride profiling of the limited number of cores available for a given structure is cost effective. Therefore, Product No. 2030 is not considered to be advantageous for application to normal FDOT marine substructure diagnostics.

Product 2029, *Effectiveness of Penetrating Sealers*

This product uses two methods (one based on electrical resistance measurements and the other on liquid absorption) to assess the condition of a penetrating sealer that has been applied on a concrete surface. The methods do provide a quick indication of the condition of the sealer. However, the applicability of this product to marine substructure diagnosis in Florida is very limited since penetrating sealers are not in common use for corrosion control purposes in the systems of interest. Therefore, assessment of this product was not conducted.

Product 2031, *Concrete (Air) Permeability*

Product 2031 is based on determination of concrete permeability by measurement of air conductance. The sampling depth of this technique is low (about 13 mm below the surface) and the method is intended for relatively dry surfaces. If surfaces were wet, they need to be heated prior to testing to drive off moisture. The method is clearly not applicable to the regions of marine substructure where corrosion severity is greatest (the splash-evaporation zone). The FDOT has developed its own in-situ permeability determination procedures for marine substructure [15], which is recommended to be considered instead of Product 2031.

Product 2015, *Ground Penetrating Radar*

Product 2016, *Deck Membrane Integrity*

These two products address exclusively condition assessment of bridge decks and are of marginal applicability to FDOT corrosion diagnosis needs. Therefore, assessment of these products was not conducted.

Product from SHRP C-103, *Life Cycle Cost Analysis Methodology*

The methodology for Life Cycle Cost Analysis (LCCA) developed under SHRP C-103 [16] represented an important development in quantitatively forecasting corrosion deterioration as a means to decide when and how corrosion protection measures will need to be implemented. The methodology was introduced to FDOT personnel as part of the FHWA Workshop of SHRP Research Products seminar series, and its implementation to serve FDOT needs became the main thrust of the present project.

The SHRP methodology consists of first assessing the condition of the structure by means of physical observation that include visual determination of spalls, delamination survey, bar cover and continuity measurements, chloride content at the bar depth, corrosion rate measurements when necessary, chloride permeability if necessary, and concrete resistivity. The results of the survey are tallied to obtain a numeric condition index S. The value of S at future times is then forecast using charts and criteria provided as part of the methodology. Based on the progression of S with time, corrosion control/rehabilitation treatments are applied whenever S exceeds a limit

provided also as part of the methodology. Charts are provided to forecast how S will progress after each treatment. The cost of each treatment is used to compute a life cycle cost and to make cost-oriented decisions to choose between alternative treatment scenarios.

The SHRP methodology is tailored to bridge deck maintenance, with empirical criteria to forecast S based on bridge-deck deterioration experience which are not applicable to marine substructure conditions. While promising, this product needed to be adapted to serve FDOT needs.

SELECTION OF PRODUCT FOR FURTHER DEVELOPMENT

Based on the review summarized above, it was concluded that the procedure for estimating residual service life under the product from SHRP C-103, *Life Cycle Cost Analysis Methodology* [16], merited further development and adaptation to FDOT needs. Development took place and resulted in the steps detailed in the next heading and further addressed in the rest of the report.

PROCEDURE FOR ESTIMATING RESIDUAL SERVICE LIFE

The SHRP LCCA methodology was subjected to substantial modification to adapt it to the marine substructure service of interest to FDOT. The adapted procedure, focusing on forecasting damage progression, involves the following steps:

1. Initial condition assessment is made by visual observation of corrosion induced cracks and spalls in the substructure. All substructure members of a given type (for example precast piles) are treated similarly. Within each member type, the surface is divided if necessary into two or more elevation zones (for example, Tidal, Lower Splash, and Upper Splash zones).
2. A random sampling scheme is established for each member type. Concrete cores (preferably 10 or more) are extracted from sound concrete of separate members at each elevation zone. A concrete cover depth survey is also conducted.
3. The cores are analyzed to obtain chloride concentration profiles from which the surface concentration and diffusion coefficient (defined in the following section of this report) are calculated for each location. The results are tabulated and used as discrete distributions, or alternatively analyzed for best fit to an ideal statistical distribution to obtain average values and standard deviation for those parameters. A similar approach is used for the cover depth data.
4. Chloride concentration threshold and corrosion propagation time parameters (see next section of this report for definitions) are selected for each elevation zone from information derived from FDOT experience. The values of those parameters together with the statistical information obtained in Step 3 are processed using the convolution formulas developed under this and related projects [17] to obtain a damage function for

the structure. The damage function gives the total m^2 of cracked/spalled substructure surface that is projected to appear as function of time during the future life of the structure (that damage function is somewhat comparable to the condition parameter S in the original SHRP LCCA methodology).

5. The damage function is the main outcome of the procedure developed here. This damage function can then be directly applied to compute life cycle cost of various treatment alternatives (or of the corresponding "do-nothing" option) using the procedure already available in the SHRP methodology. Treatment alternatives for marine substructure include simple patching, fiberglass-formed cementitious jackets with sacrificial zinc anodes, sprayed zinc anodes, impressed current cathodic protection, use of stainless steel reinforcement in repaired patches, etc. Each alternative has a cost associated with it, which is inserted in the LCCA calculation. Each alternative has also a useful life limit and repeated application needs to be costed if the life limit of the alternative is less than the remaining service life of the structure. Selection between alternative treatment strategies can then be made based on LCCA output and FDOT service need criteria. Because LCCA procedures given a specific damage function are already well established, they have not been further developed in the present project.

The detailed approach used to implement steps (1) through (4) above is contained in the following sections.

4. DAMAGE PROGRESSION MODEL

STATEMENT OF THE PROBLEM

Predicting damage progression with time (the "damage function") in reinforced concrete structures subject to corrosion damage is important to design and maintenance. Reliable methods for corrosion forecasting are especially desirable for service applications that involve exposure to chloride ions, which affects a large part of the worldwide transportation infrastructure. The task, however, is made complicated by the variability of exposure and materials conditions existing within even a small structure. This complication notably affects marine bridge substructure where chloride transport regimes change dramatically with elevation above sea level. A general approach to corrosion damage forecasting under distributed conditions is presented here, together with two specific illustrations for marine systems.

The simplest corrosion forecasting involves a two-step approach [18]. In the first step (initiation), the chloride ion concentration at the steel surface is initially below the critical threshold C_T for appearance of active corrosion of the steel. The concentration, however, is increasing with time because of chloride transport through the concrete cover. The initiation period ends when the chloride concentration at the rebar surface reaches the value C_T . During the propagation period corrosion products accumulate. The propagation period ends with the development of concrete cover delamination spalls, appearance of concrete cracks, or similar manifestations of distress.

The length t_i of the initiation period can be evaluated with appropriate information and assumptions on the mechanism of chloride transport and value of the transport parameters, and on the value of C_T . The length t_p for the propagation period can be estimated from materials and environmental properties as indicated later, or assigned a nominal value based on prior experience. In a structural element with uniform concrete cover, concrete and rebar properties, and exposure conditions, the damage function would take the form of a step: damage is unobservable (or below some acceptable limit) before $t_i + t_p$, and damage is observable (or exceeding some tolerable limit) afterwards. The element would then experience a sudden transition from not being distressed to being declared as distressed. However, experience shows that in actual structures distress is observed (or exceeds a given limit) at different times for different elements within the structure, leading to gradual development of damage for the entire system. This behavior may be envisioned as resulting from the superposition of numerous individual step functions corresponding to the end of the propagation stage of different portions of the structure, each with its own values of chloride transport, corrosion initiation, and corrosion propagation parameters.

GENERAL APPROACH TO MODELING DISTRIBUTED BEHAVIOR

The main premise in the approach outlined here is that the structure exposed to corrosion risk can be divided into a large number of individual elements of equal size,

traced on the concrete surface, such that the corrosion initiation and propagation processes within each element are independent of those in any other element. The element size is assumed to be small enough that the concrete and reinforcement properties, as well as the concrete cover and surface exposure conditions, may be considered to be uniform. On the other hand, the element size is assumed to be large enough that when corrosion propagates and damage is eventually made visible in the form of concrete cracking or delamination, the damage does not extend into neighboring elements.

Parameters of importance within each element to defining the length of the corrosion initiation stage may include properties such as C_T , the clear concrete cover x , the apparent chloride ion diffusivity D , and the chloride concentration at the concrete surface. The length t_p of the propagation stage may be on first approximation assumed to be a fixed value. However, in a more sophisticated treatment (as in Section 6 of this report) t_p may be considered instead to be proportional to the ratio of x to the rebar diameter Φ [8]. The proportionality factor $k = t_p \Phi/x$ may be also assigned a dependence on corrosion rate, or on the condition of the coating when coated rebar is used. If only the variables just assigned symbols were of importance, the total time to developing externally observable distress, t_s , on an element could be expressed as

$$t_s = f(x, D, C_s, C_T, \Phi, k) \quad (1)$$

If the values of all the parameters other than x were kept the same, then the value x_s of x that results in distress appearing at time $t_s \geq t_p$ could be expressed as a function of the other parameters such as:

$$x_s = F(t_s, D, C_s, C_T, \Phi, k) \quad (2)$$

The actual form of functions f and F depends on the chloride transport, initiation and propagation models, and number of relevant variables assumed. Examples of those forms will be presented in the following sections.

For a more general treatment, a series of variables $V_1 \dots V_n$ can be considered where $V_1 = x$, and V_2, \dots, V_n represent all the other relevant factors or parameters affecting corrosion initiation and propagation. Thus a more general form of Eqs. (1) and (2) is:

$$t_s = f(V_1, \dots, V_n) \quad (3)$$

$$V_{1s} = F(t_s, V_2, \dots, V_n) \quad (4)$$

In an actual structure all these parameters are subject to variability that can be both systematic (for example decreasing C_s with elevation above sea level in marine bridge substructure) and probabilistic (such as changes in D with batch-to-batch

variations in concrete mixture proportions, or with concrete placement quality). Thus, it will be assumed that the structure can be divided into separate regions (for example elevation ranges) such that within each range the values of variables $V_1 \dots V_n$ obey independent probability distributions with parameters that depend on the region considered. In the following, regions will be numbered 1,2 i Nr, and elements within each region will be numbered 1,2.... j...Ni.

Thus the probability that the value of parameter V_k in element j within region i is within an interval dV_k wide around the value V_{kij} is $P_{ki}(V_{kij}) dV_k$, where P_{ki} is the probability distribution function for variable V_k in elevation range i. As the probability distribution functions are assumed to be independent of each other within a given region, the probability of finding a combination of values (within specified intervals) of different parameters in a given element is simply the product of the individual probabilities. For a structure containing an arbitrarily large number of elements, the probabilities thus evaluated represent the fraction of elements having the specified combination of parameters.

It will be further assumed that both the mechanisms of corrosion initiation and propagation are such that, if all the other variables are constant, distress will always be manifested first in the element with the least concrete cover. This assumption is consistent with diffusional chloride ion transport through the concrete cover, and with the observation that generally less steel corrosion is required to cause cracking of the concrete when the concrete cover is smaller [8,19]. Consider now within region i a set of elements that may have variable values of parameter V_1 (the steel cover x), but that share the same values for the remaining parameters $V_2 \dots V_n$ within infinitesimal intervals $dV_2 \dots dV_n$. Per the latest assumptions, at time t_s (Eqs.(1-4)) any elements within that set having $V_1 \leq V_{1s}$ will already have experienced distress. The fraction of elements in the set satisfying that condition is obtained by integrating the V_1 probability distribution up to V_{1s} , yielding $\int_0^{V_{1s}} P_{1i}(V_1) dV_1 = P_{cum1i}(V_{1s})$, the cumulative probability for V_{1s} . V_{1s} is in turn equal to $F(t_s, V_2, \dots V_n)$ per Eq.(4). Thus, the fraction of elements in region i that belong to this set and that have also experienced distress by time t is:

$$dNi(t)/Ni = P_{cum1i}(F(t, V_2, \dots V_n)) P_{2i}(V_2) \dots P_{ni}(V_n) dV_2 \dots dV_n \quad (5)$$

Integrating now over all the possible parameter values in each region and adding up the results of all regions yields the fraction $Ns(t)/N$ of elements over the entire structure that have experienced distress by time t_s :

$$Ns(t)/N = (1/\sum_i Ni) \sum_i Ni \int_{V_2} \dots \int_{V_n} P_{cum1i}(F(t, V_2, \dots V_n)) P_{2i}(V_2) \dots P_{ni}(V_n) dV_2 \dots dV_n \quad (6)$$

Eq.(6) then represents the progression of corrosion distress in the structure as function of time, which can be projected if one has knowledge of the distributions P_{ki} and the function $F(t_s, V_2 \dots V_n)$. Application of this approach to actual systems with significantly different corrosion forecasting needs is illustrated in the following sections.

5. CASE APPLICATION - ESCAMBIA BAY BRIDGES

CASE STATEMENT

The parallel twin Escambia Bay bridges were built in 1966 to span Escambia Bay near Pensacola, Florida. The water in contact with the bridges has a variable chloride content, with concentrations exceeding 10,000 ppm at times. In 1996 the FDOT began reviewing alternatives for upgrading these bridges, including widening or replacing the bridges. To assist in deciding between alternatives, an assessment of the corrosion condition of the bridges and a forecast of future deterioration were conducted under a separate investigation [17], where a precursor of the general modeling approach introduced in the Section 4 was applied. This section reproduces, as a methodology illustration, some of the material published by the author and collaborators in Ref. [17]. For this report, some of the model application aspects have been reformulated in terms of the general equations presented in Section 4.

Each bridge is 4.1-km-long (2.5-mi-long), with 223 substructure bents. The bents in the higher elevations of the bridges are comprised of 268, 1.37-m (4.5-ft) diameter Raymond piles. Smaller diameter 0.91-m (3-ft) Raymond piles (1,218 in water) support the lower elevations of the bridges. Connecting struts that were to be replaced in any event, and a small number of crash walls were addressed separately and will not be further considered here.

Evaluation of the bridges at age 31 years was conducted by Concorr Inc. [20] and relevant findings are reproduced here. The evaluation included a comprehensive condition survey which consisted of visual observation, direct examination of reinforcement, electrochemical corrosion measurements, concrete cover measurements, and determination of chloride ion penetration profiles. No corrosion-induced damage or deterioration of the 31-year-old round piles was identified. The clear concrete cover of the piles (average of 2.84 cm (1.12 in) for 47 test spots and 2.64 cm (1.04 in) for 14 test spots in the 0.91-m (3-ft) and 1.37-m (4.5-ft) piles, respectively) corresponded to the spiral stirrup wire wrapped around the longitudinal prestressed cables. The cover measurements were performed by direct observation in drilled holes.

For electrochemical and chloride penetration assessment, tests were performed at three elevations corresponding to the tidal zone (TZ), about 0.15 m (0.5 ft) below high tide elevation (-0.15 m (-0.5 ft) above high tide, AHT), the upper splash zone (US), about 0.75 m (2.5 ft) AHT for the 0.91-m (3-ft) piles and 1.2-m (4-ft) AHT for the 1.37-m (4.5-ft) piles, and the above-splash zone (AS), about 1.5 m (5 ft) AHT.

Nominal corrosion rate measurements were made with a Gecor 6 test device at 41 pile locations selected to minimize sampling bias and representing the three elevation ranges indicated above. Average nominal corrosion current densities for both types of pile in the TZ, US and AS zones were in the range normally associated with low or negligible corrosion rates of steel in concrete [21]. Chloride concentration profiles

were obtained successfully at 17 unbiased sampling locations in the three elevation regimes indicated above. The results, discussed in detail below, indicated that at the time of the survey the chloride concentrations in the US and AS zones at the depth of the stirrup wire were below (but near), and in the TZ were above, the value (typically on the order of 1 kg of Cl⁻ ions per m³ of concrete) normally associated with the onset of active corrosion of steel in concrete [22].

The results of the survey indicated that the corrosion condition of the piles was very good, especially considering the high Cl⁻ content of the water, the bridge age, and the low concrete cover thickness. However, the chloride profile results suggested that corrosion initiation had possibly already started in the TZ and was likely in the near future for the US and AS zones.

SPATIAL DISTRIBUTION AND DETERIORATION MODEL

The bridge round-pile substructure was divided into three elevation regions designated by $i=1$ (tidal, T); $i=2$ (lower splash, LS) and $i=3$ (combined upper splash and above-splash, US-AS). The LS range was introduced as an artificial intermediate range of average properties between those of the T and the LS-US ranges, to address a region of possible early deterioration. The minority of piles with surrounding struts was treated conservatively as if the struts offered no resistance to chloride penetration. Each elevation region was assigned N_i surface elements ($1, 2, \dots, j, \dots, N_i$) of equal area A_e . N_i included the elements of both twin bridges.

Each element j in range i was assumed to have a concrete rebar cover $x_{i,j}$. Chloride ions were assumed to be transported by near-flat geometry Fickian diffusion, with an apparent chloride ion diffusion coefficient D_{ij} invariant with time for each element. The surface chloride ion concentration of each element was also assumed to have a time-invariant value $C_{s,i,j}$. The native chloride content of the bulk concrete was assumed to be the same throughout the bridge and negligibly small for the purposes of this model. The chloride concentration threshold C_T was assumed to be the same for all the elements within each elevation region. Likewise, the corrosion propagation time was assumed to be the same, $t_{p,i}$, for all elements within each elevation region i .

The above assumptions imply then that the ruling parameters for Eqs.(2-3) are: $V_1=x$; $V_2=C_s$; $V_3=D$; $V_4=C_T$; $V_5=t_p$, of which only V_1 , V_2 and V_3 are distributed while V_4 and V_5 are constants within each region. Under simple near-flat diffusion with constant surface concentration and negligible native content, the chloride concentration at depth x and time t is given by

$$C(x, t) = C_s \left(1 - \operatorname{erf} \frac{x}{2\sqrt{Dt}} \right) \quad (7)$$

Therefore the condition to achieve corrosion initiation is $C(x, t_s) = C_T$ which per Eq.(7) means then that the function f adopts the form:

$$ts = \frac{x^2}{4D \left(\operatorname{erf}^{-1} \left(1 - \frac{C_T}{C_S} \right) \right)^2} + tp \quad (8)$$

or:

$$ts = \frac{V_1^2}{4V_3 \left(\operatorname{erf}^{-1} \left(1 - \frac{V_4}{V_2} \right) \right)^2} + V_5 \quad (9)$$

Likewise, the function F adopts the form

$$x = 2\sqrt{D(ts - tp)} \operatorname{erf}^{-1} \left(1 - \frac{C_T}{C_S} \right) \quad (10)$$

(for $t > tp$)

Thus Eq.(6) for this case takes the form:

$$\frac{Ns(t)}{N} = \frac{1}{\sum_i N_i} \sum_i N_i \int_{D_{li}}^{D_{hi}} \int_{C_{sli}}^{C_{shi}} P_{\text{cumx}} \left(2\sqrt{D(ts_i - tp_i)} \operatorname{erf}^{-1} \left(1 - \frac{C_T}{C_S} \right) \right) P_{C_{si}}(C_S) P_{D_i}(D) dC_S dD \quad (11)$$

where D_{li} , C_{sli} and D_{hi} , C_{shi} represent the lowest and highest values respectively of D and C_s in elevation range i . The total projected damaged surface area $S(t)$ in the substructure at age t is then:

$$S(t) = Ns(t) A_e \quad (12)$$

MODEL IMPLEMENTATION

To calculate the projected damage function the following input parameters were required for each elevation range i (except for A_e , which is global) and obtained as follows:

- A_e : Chosen to be 0.1 m^2 (1.1 ft^2), representing typical expected repair patch sizes (same for all elevation ranges).
- N_i : Obtained from A_e , pile dimensions, the number of piles of each type and the elevation range limits as shown in Table 1. The T ($i=1$) elevation range extended from the high tide (HT) level to 0.45 m (1.5 ft) below, reflecting the typical tidal variation in Escambia Bay. The LS ($i=2$) elevation range extended from HT to 0.3 m (1.0 ft) above high tide (AHT). The US+AS ($i=3$) range was from 0.3 m (1.0 ft) AHT to 1.8 m (6.0 ft) AHT. Elevations higher than 1.8 m (6.0 ft) AHT were assumed to result in negligible corrosion development in the time frame of interest.
- C_{Ti} : Chosen to be representative of the concrete and rebar conditions as shown below. Assumed to be $M \cdot CF$ at all three elevation ranges. CF is the cement factor of the concrete used in the piles. M is a multiplier which is often assumed to be 0.004 for design purposes [23]. However, because of uncertainty in this parameter for marine substructures in Florida, three alternative cases A, B, and C were evaluated with $M= 0.004, 0.008$ and 0.012 , respectively. Using $CF = 400 \text{ kg /m}^3$ (674 pcy) resulted in $C_{Ti} = 1.6 \text{ kg/m}^3$ (2.7 pcy), 3.2 kg/m^3 (5.4 pcy) and 4.8 kg /m^3 (8.1 pcy). Within each alternative projection, C_{Ti} is the same for $i=1, 2$, and 3 .

P_{Cs_i} (Cs),

P_{D_i} (D),

P_{cumCi} (x):

These distribution functions were approximated by fitting the measured populations to ideal normal distributions truncated as appropriate. Each distribution required four parameters: the average, the standard deviation, and the upper and lower truncation limits.

For the Cs and D distribution functions, a concrete unit weight of $2,547 \text{ kg /m}^3$ (4,290 pcy) was used to convert chloride concentrations from percent by weight of concrete to kg/m^3 (pcy). Based on measurements at depths of $\approx 10 \text{ cm}$ (4 in), the native chloride content was assumed to be $\approx 0.12 \text{ kg/m}^3$ (0.2 pcy). Figure 1 shows the values of D and Cs as a function of elevation obtained by analysis of 17 extracted cores from both types of piles. There was no significant evidence of different trends for the 0.91-m (3-ft) and 1.37-m (4.5-ft) piles. Both Cs and D tended to be higher in the T range than in the US and AS ranges. The results of the two latter ranges were not clearly differentiated and were consequently grouped together. Table 2 presents the average and standard deviation values of D and Cs for each of the two distinct groups thus identified. The populations of both groups (especially that for the Tidal regime) are small, so the standard deviation values can only be considered as nominal values. Nevertheless, at least for the US + AS regimes, there is reasonable approximation between an ideal normal distribution and the actual cumulative value counts, as shown in Figure 2. Nominal parameter values were assigned for the LS zone and listed in

Table 2. These values were intermediate between those for $i=1$ and $i=3$ and chosen to follow, at an elevation of .15 m (0.5 ft) AHT, the general trends of Figure 1.

For the x distribution function, direct measurement of the concrete cover in the 0.91-m (3-ft) and 1.37-m (4.5-ft) piles yielded similar results, as shown in Table 3. The spiral pitch is only ≈ 7.5 cm (3 in) (design detail drawings), resulting in a large amount of stirrup steel. It was then expected that the first corrosion-related damage requiring extensive repair will be from the spiral hooping. Since the piles were precast, the same values (overall average = 2.79 cm (1.1 in); standard deviation = 0.63 cm (0.25 in)) were used for $i = 1$ to 3. No distinction was made between 0.91-m (3-ft) and 1.37-m (4.5-ft) piles. Figure 3 shows the cumulative distribution of stirrup cover values for the 0.91-m (3-ft) piles, compared with an ideal cumulative normal distribution having the average and standard deviations for those piles. The resolution of the field measurements was ≈ 6 mm (0.25 inch). No values lower than 1.9 cm (0.75 inch) were recorded for any of the stirrup measurements in either the 0.91-m (3-ft) or 1.37-m (4.5-ft) piles. In an ideal normal distribution with the parameters for Figure 3, 0.85% of the stirrup measurements (less than 1 in a field of 47 tests) would have been 1.27 cm (0.5 inch) or less. Thus, the absence of lower readings in the present sampling is not by itself statistically indicative that the concrete cover in the stirrups was limited by construction to 1.9 cm (0.75 in). However, some form of cover limitation (for example, by the use of form saddles) was likely in the precast procedure. Moreover, corrosion damage was not conspicuous anywhere in the 1,486 piles on water after 31 years of service. Consequently for the purposes of the model, the distribution was truncated at 1.9 cm (0.75 in).

tp_i : In the absence of corrosion measurements of confirmed active steel, the value of tp_i for elevation ranges 2 and 3 was assigned to be 7 years ($2.2 \cdot 10^8$ sec). Because of the apparent high concrete quality, this value was twice the nominal value used in previous estimates of durability for FDOT bridges. The value assigned to tp_i in the T elevation range was 30 years ($9.5 \cdot 10^8$ sec), an assumption based on the expectation of much lower corrosion rates in the tidal region where very slow oxygen transport is expected.

CALCULATION AND MODEL OUTPUT

Once the input parameters were available, the calculations were conducted with a MATHCAD worksheet. The distribution functions were calculated first. Equation [11] was implemented as a double summation with (typically) 20 terms per summation. Additional terms yielded only minor changes in output while extending computation time considerably. The program output was the extent of damaged area (m^2 added for the two bridges) at each of the three elevation ranges as a function of time since construction. Results were presented at intervals of 5 years, up to a service life approaching 100 years.

Figures 4, 5 and 6 show the model output for Cases A, B and C (C_T equal to 1.6, 3.2 and 4.8 kg/m³, respectively). The amount of damage (total for the two bridges) is given in m² by the value of $TS1_k$, $TS2_k$ and $TS3_k$ for elevation regimes $i=1$, $i=2$ and $i=3$ respectively. The sum of the damage in the three regimes is given by TSA_k .

The model outputs show a period of no significant corrosion damage followed by the gradual development of deterioration afterwards. The shape of the curves for each elevation range reflects the assumed dispersion of model parameters (concrete cover, surface concentration, and diffusivity) around their respective average values. An assumption of no dispersion would have resulted in a sharp step damage function for each range, with damage starting at the time corresponding to that dictated by the average parameter values plus the assumed propagation time. The model outputs project the most damage taking place in the Tidal zone during the decades following the time of examination of the structures.

The projected bridge age for observation of significant corrosion was about 20 years for the most conservative of the alternative cases ($C_T = 1.6$ kg/m³ (2.7 pcy), Case A), and almost 40 years for the least conservative Case C. Thus, these alternatives bracket the observed absence of significant damage when the structures were examined at age 31. In all 3 realizations the total projected damage reached 1000 m² (10,764 ft²) some 20 years after the first appearances of significant damage. Detailed cost estimates for rehabilitation were prepared and reported elsewhere [20] based on the repair/rehabilitation alternatives considered [2].

6. CASE APPLICATION - FLORIDA KEYS BRIDGES BUILT WITH EPOXY COATED REBAR

CASE STATEMENT ^B

Epoxy-coated rebar (ECR) has been used in approximately 300 Florida bridges, principally in an attempt to control corrosion of the substructure in the splash-evaporation zone of marine bridges. Starting in 1986, severe corrosion of ECR began to be observed in five major bridges built between 1978 and 1983 along US 1 in the Florida Keys [12,21,25]. The development of corrosion damage has been recorded periodically. An update for the first 20 years of structural service life is presented here.

Table 4 lists the structures affected, nomenclature, and construction information. Three of the bridges (7MI, NIL and INK) were built with drilled shafts supporting columns with connecting struts. The LKY bridge had capped drilled shafts joined by a strut, and V-Piers rested on synthetic rubber pads placed on the caps. The CH5 bridge had drilled shafts with spread footers and precast, post tensioned box columns.

Unless indicated otherwise, the concrete used in the substructure was cast in place (CIP) and conforming to FDOT Class IV specifications at the time of construction. Those specifications established $w/c < 0.41$, cement content = 388 Kg /m^3 (658 lb/yd^3) and 28-day strength $> 23.5 \text{ MPa}$ ($3,400 \text{ psi}$). The fine aggregate was sand and the coarse aggregate oolitic limestone. The cement type for each structure is indicated in Table 4. The specified maximum chloride content (acid soluble test) for concrete in these structures was 0.24 kg/m^3 (0.4 lb/yd^3). The design clear rebar concrete cover for the substructure of these bridges was 76 mm (3 in). Substantial deviations from that value were often observed, especially in round columns when the rebar cage was not precisely centered. As a result, it was not uncommon to encounter concrete cover as little as 25 mm (1 in) on one side of the column and 125 mm (5 in) on the other side. Some instances of no cover were encountered.

Initial chloride content of the concrete in the bridges (from FDOT records) was small for NIL, LKY and CH5, but that it was considerably higher for 7MI (1.8 kg/m^3 (2.9 lb/yd^3)) and INK ($0.7 - 2.1 \text{ kg /m}^3$ ($1.1 - 3.5 \text{ lb/yd}^3$)). It has been speculated that the higher values reflected seawater contamination of the coarse aggregate.

The ECR had been manufactured and coated following ASTM 775 - 76 and ECR placement guidelines in place at the time of construction [26,27]. Those guidelines allowed a maximum of 2% unrepaired surface damage at rebar surface. The coating material and applicators for each bridge are listed in Table 4. Rebar sizes ranged from #3 (10 mm diameter) to # 8 (25 mm). Rebar tie wires, as revealed by direct examination, were bare steel.

Conventional patch repairs and corrosion control procedures were conducted at various times in selected bents (piers) of these bridges. The most notable protective

^B Portions of this section have been published during the development of this project [24].

procedure was installation starting in 1988 of sacrificial sprayed-zinc anodes [28] at LKY (38 bents by 1996 plus 30 bents by 1998), NIL (31 bents by 1996), and 7MI (148 bents by 1998). In some instances the anodes were supplemented by immersed bulk anodes [28]. Information being compiled at this time indicates substantial corrosion mitigation in the elements protected by this method. Other procedures included patching with concrete incorporating corrosion inhibiting admixtures, bar coatings, and proprietary cementitious repair mortars. The effect of these procedures is being evaluated.

Examination of the structures was conducted at various levels. A general visual examination, performed periodically, was made by an experienced crew travelling slowly by boat and examining the entire perimeter of each bent in the bridge. If evidence of cracking or other distress was observed, the substructure element was tested by sounding with a hammer for evidence and extent of internal delamination. An area of delaminated concrete thus detected was designated as a concrete spall. A delaminated area which extended from an area found to be spalled in a previous inspection was designated as a progressive spall. On selected bents, the delaminated concrete was removed to expose the ECR and directly determine the extent of corrosion. Chloride ion (acid soluble) concentration profile measurements were conducted on cores extracted from selected bents.

Table 5 lists the results of visual and sounding examinations performed between 1986 and 2000. The number of new spalls or progressive spalls observed on a bridge at a given inspection date was recorded. That number was then added to those observed in the previous inspections of the same bridge, and reported in Table 5 as the cumulative number of spalls to the listed date. Spalls that occurred in regions formerly repaired (either by conventional patching or otherwise) were considered a new spalls.

Typical spalls affected a projected area of $\sim 0.3 \text{ m}^2$ ($\sim 3 \text{ sq.ft.}$) on the surface of the concrete. Although rust stains were present on the delaminated surface, much of the epoxy coating was still visible on the rebar. Longitudinal cuts with a sharp knife permitted easy peeling of the coating from the corroded regions, revealing extensive corrosion products underneath. Those internal corrosion products were generally solid, dark, magnetic and electronically conductive [29]. Occasionally, significant amounts of acidic liquid rich in chloride and iron were found as well [12,30].

Sandblasting of the corroded region to remove the epoxy and corrosion products revealed that extensive metal loss had occurred, in the form of pits several mm long and deep. In some instances, corrosion-free steel tie wire was found in contact with corroding regions of the ECR.

The coating on rebar adjacent to and also away from the corroding region was found to be easy to peel after cutting with a knife, revealing bright or slightly darkened metal underneath. This disbondment without significant corrosion was found to be widespread in ECR after it was in service for a few years in Florida marine substructure conditions, even in the absence of chloride contamination of the concrete next to the rebar [25,31]. Examination of the underside of coatings from numerous ECR samples

from Florida bridges did not reveal any correlation between this disbondment and the usual forms of surface contamination expected in the coating process [25,31].

Chloride ion profiles indicated that extensive chloride penetration of the concrete had taken place in the splash zone of the structures affected. At the time of the first spall observations, chloride content at a depth of 50 mm to 76 mm in the splash zone of LKY, 7MI and NIL was between 8 kg/m^3 (14 pcy) and 14 kg/m^3 (24 pcy) [25]. D values determined from the chloride profiles for the splash zone in those bridges ranged from $\sim 10^{-8} \text{ cm}^2/\text{sec}$ ($\sim 0.1 \text{ in}^2/\text{y}$) to as much as $\sim 6 \cdot 10^{-7} \text{ cm}^2/\text{sec}$ ($\sim 3 \text{ in}^2/\text{y}$) [25,32]. These high diffusivities agreed with concrete resistivity readings as low as $\sim 1 \text{ k}\Omega \text{ cm}$ in the tidal region [25,33,34].

ACTUAL CORROSION PROGRESSION

To compare the progression of corrosion in bridges of different lengths, the data in Table 5 were normalized by dividing the number of spalls by the number of bents in each bridge. The resulting damage functions (spalls per bent as function of time) are plotted in Figure 7. The corrosion damage after nearly 20 years of service is conspicuous (more than one spall per bent) and affects a significant fraction of the area of the splash zone of each bridge (the concrete surface area on the splash zone of a typical bent is $\sim 20 \text{ m}^2$ while a typical spall affects $\sim 0.3 \text{ m}^2$). Damage is likely to have been worse without the application of protective anodes. Except for an offset toward shorter times for NIL, the functions are remarkably similar to each other. The damage at present appears to increase approximately linearly with time. If those trends were to continue, the total extent of damage would roughly double over the next 20 years of service. As repairs in marine substructure are very costly, corrosion would place a continuing and heavy repair and maintenance burden during the service life of these structures.

DETERIORATION MODEL

The appearance of the damage functions in Figure 7 clearly indicates that the development of damage was gradual and amenable to an interpretation based on distributed variables. The modeling approach introduced in Section 4 was adapted to the present case for future behavior projection and also to provide insight on the factors responsible for damage development in the past. For simplicity, the impact of corrosion control procedures in the observed damage functions was ignored.

MODEL INPUT PARAMETERS

As in the previous application, precise knowledge of the parameters relevant for damage development in these structures is not available. However, insight on the factors responsible for the corrosion progression was sought by assuming parameter values and variabilities typical of these structures. As indicated above, D values are large and a value equal to $2 \cdot 10^{-7} \text{ cm}^2/\text{sec}$ may be considered to be typical. For bridges in this group, the value of C_s typically reached $\sim 14 \text{ kg/m}^3$ [25] at the bottom of the

splash evaporation zone and decreased with increasing elevation (because of the high diffusivity, concentration values at the rebar depth often approached those at the surface after only a few years of operation). This condition may be approximated by a normal distribution truncated at the nominal average value. The design value of x (76 mm), and the range of variation of x (0 to 160 mm), are known from specifications and can be estimated from field observations respectively. Laboratory observations suggest that under simple conditions C_T for ECR is on the order of the value for plain steel bar [25]. As in the previous Section, C_T was estimated as being proportional to the cement content (CF) of the concrete. A single case with $C_T \sim 0.004$ CF [23] (the middle of the three choices investigated in the previous Section) was assumed.

As will be shown below, the corrosion propagation stage in these structures appears to dominate much of the damage development. Consequently, a more refined approach than in the previous Section was used here to assign values to t_p . There is growing evidence that, for a given corrosion rate and rebar size, t_p of conventional rebar (and likely also for ECR) is directly proportional to x [19]. For a particular value of x and Φ , t_p should be longer as the rebar corrosion rate is smaller [19]. The corrosion rate (averaged over the bar surface) is strongly influenced by the condition of the coating [35,36]; ECR with substantial coating distress should corrode faster than in the absence of imperfections. Thus for modeling purposes, the propagation time for this application was expressed as $t_p = k' x$, where $k' = k / \Phi$ is a parameter that becomes smaller as the extent of ECR coating distress increases (for simplicity Φ was assumed to be same for all the rebar in the affected regions). Under those conditions the value of t_s is given by:

$$t_s = \frac{x^2}{4D \left(\text{erf}^{-1} \left(1 - \frac{C_T}{C_s} \right) \right)^2} + k' x \quad (13)$$

and the function F adopts the form:

$$x = -\frac{k'P}{2} + \frac{1}{2} \sqrt{k'^2 P^2 + 4 t_s P} \quad (14)$$

$$\text{where } P = 4D \left(\text{erf}^{-1} \left(1 - \frac{C_T}{C_s} \right) \right)^2 \quad (15)$$

Replacing F in Eq.(6) then yields the corresponding damage function for the fraction of the surface having a given value of k' .

Variability in the values of x , D and C_s was idealized as before by normal distributions, truncated as appropriate. Variability in t_p was introduced in the model through the parameter k' as indicated below, an approach that produced plausible results when used together with the value of C_T indicated above.

Table 6 lists the parameter values used for model inputs, based on the typical values indicated earlier.

CALCULATION AND MODEL OUTPUT

The average input parameter values in Table 6 were based on the typical conditions indicated above, while the variabilities represent typical conditions observed in marine substructure and representative also of those encountered in the previous application. The calculations assumed initially chloride-free concrete. The assignment of k' values over the rebar assembly, which was treated for simplicity as a discrete distribution, assumed that only a small fraction (2%) of the rebar assembly was responsible for the earliest observations of damage. That fraction had a low value of k' (0.14 y/mm, which results in $t_p=7$ years when $x=50$ mm) and consequently was responsible for the very first failures projected. Increasingly large fractions of the assembly were assumed to have correspondingly larger propagation times. This approach is based on the expectation that rebar segments with a high incidence of coating distress are likely to have the highest corrosion rates and therefore the shortest t_p values. The chosen distribution for k' then effectively states that there was a small fraction of the rebar with severe coating distress, and proportionally less distress on increasing fractions of the assembly. Figure 8 shows the model output. The effect of the model assumptions is apparent in the dashed lines of Figure 8, which show the contribution to the total damage from each of the distress fractions assumed.

The choice of input parameters used yielded a projected damage evolution for the first 20 years that was consistent with the observed behavior in Figure 7. The projection reasonably reproduced the duration of the initial period with minimal damage, and the subsequent steady rise at a rate of ~ 0.1 spall/bent/year observed in the bridges. Sensitivity tests showed that the damage projection was only modestly influenced by changes in the distribution of D or C_s , or by variations in C_T . This behavior is a consequence of the severe exposure regime assumed, which causes the corrosion threshold to be reached at much of the rebar surface very early in the simulation. A similar circumstance may account in the actual structures for the little differentiation (Figure 7) between the trends in 7MI and INK, which had initial chloride contamination, and that of the other bridges. Thus the projected behavior was determined mainly by the corrosion propagation phase, which depended strongly on the k values and cover distribution assumed. It was felt that the chosen value for the variability of x (described by the parameter s_x in Table 6) was reasonably representative as it allowed for $\sim 10\%$ of the cover to be less than 5 cm, reflecting several observations of low cover during inspection of the first recorded spalls. The k' distribution chosen for Table 3 was only a working example. However, ranging calculations confirmed that reasonable fit to

observed behavior could be obtained only if the percentage of the assembly assigned low k' values (yielding t_p values of only a few years) was quite small.

While exploratory in nature, the model projections for these bridges provide some insight as to possible future behavior if the actual systems. As shown in Figure 8, as time progresses the projected damage is dominated by fractions with increasingly greater k' . Whether future damage will continue along the present trend depends, in this scheme, on the extent of coating distress on the rest of the rebar assembly. If the remaining rebar coating were in very good condition, damage would continue for some time at the present rate and then saturate at some intermediate level. In the case of the values assumed for Table 3, there was no k' value assigned beyond the first 14% of the rebar assembly, and damage would saturate at ~9 spalls per bent. If the condition of the remaining rebar were poor or marginal, damage progression would not saturate soon, and could even accelerate.

7. DISCUSSION OF CASE APPLICATIONS

The case applications presented in this report exemplify typical challenges encountered when attempting to predict corrosion-limited durability of marine substructure. The deterioration models used in each case were not absolute prediction tools. Instead, the models should be viewed as means of providing quantitative projections to assist in comparing repair and future construction alternatives (for the Escambia Bay Bridges), or as means to understanding what are the mechanisms of deterioration in action (for ECR construction). In that context, the modeling approach presented here represents a significant improvement over analyses based on the behavior of single elements with a simple step damage function [40]. The benefits of a distributed parameter treatment has been well established by other investigators [32,38,39]. This methodology, with appropriate adaptation to specific needs, is therefore recommended for implementation in FDOT damage projections and analysis of cost-benefit alternatives for existing and new structures.

Much room for improvement remains. As illustrated by the results from cases A through C for the Escambia Bay Bridges, the output was highly sensitive to the assumed value of key parameters, such as the value of the concentration threshold, which are subject to much uncertainty. The overall modeling assumptions involved also numerous simplifications that ignored important issues such as (to name a few) effective diffusivity and surface concentration variations with time [40], the effect of chloride ion binding on diffusion [41,42], alternative chloride transport mechanisms [43], effect of potential on C_T [44], non-flat surfaces [8,42,45], and the factors altering the length of the propagation stage [19]. Improvement is also needed to discern between actual variability and measurement uncertainty in the parameters (concrete cover, diffusivity, surface concentration) that were used as distributed values.

An additional degree of sophistication was incorporated in the model for the structures built with ECR by including dependence of propagation time on concrete cover. Nevertheless, many other simplifying assumptions remained. Notable among the many issues not addressed in this application are the possibility of alternative C_T regimes for ECR as reported elsewhere [32]. As in the case of the Escambia Bay bridges, the effect of rebar potential on C_T was ignored. Such effect could be especially important in the Florida Keys bridges as concrete resistivity there tends to be low [25], leading to efficient coupling of still passive steel with nearby anodic regions [37]. Such coupling could lead to substantial elevation of the value of C_T of the passive steel [46] with consequent retardation of corrosion initiation and dramatic alteration of the calculated the damage projection. Comparison with the behavior of similar systems with uncoated rebar is also needed. Next generation models are beginning to address those issues, as well as incorporating the effect of corrosion protection measures such as sacrificial anodes [2,46]. The analysis presented for the ECR application underscores the importance of continuing characterization and damage development monitoring in the Florida Keys bridges, to improve understanding of the critical factors responsible for their deterioration.

8. CONCLUSIONS

1. Of the C-101 SHRP products only Product 2001, Corrosion Rate Devices appears to hold significant promise of direct application to marine substructure corrosion assessment. One of the test devices appears to be reasonably suitable for implementation of the technology. Procedures already in place at FDOT are more adequate for chloride profiling of marine substructure than Product 2030, Field Chloride Content. The other C-101 products address primarily specialized bridge deck corrosion assessment situations. The procedure for estimating residual service life under the product from SHRP C-103, *Life Cycle Cost Analysis Methodology*, was found to merit further development and adaptation to FDOT needs.
2. Development starting from the C-103 procedure for estimating residual service life showed that quantitative projections of future deterioration and interpretation of historical damage development can be performed by taking into account the compounded variability of concrete cover, chloride diffusivity, and chloride surface concentration in the substructure of marine bridges. The projected damage functions reflected the dispersion of the assumed controlling model variables. The model approach is not an absolute prediction tool, but should be viewed instead as a means to assist in comparing design alternatives.
3. The procedure developed under the present project is recommended for use in estimating corrosion-related damage progression in the substructure of marine bridges in the FDOT inventory. Areas for future improvement of this methodology include accounting for effective diffusivity and surface concentration variations with time, the effect of chloride ion binding on diffusion, the effect of rebar potential on corrosion threshold, and a more precise evaluation of the length of the corrosion propagation stage.

9. REFERENCES

- [1] Gannon, E., and Cady, P., "Condition Evaluation of Concrete Bridges Relative to Reinforcement Corrosion", Volumes 1 to 8, SHRP-S/FR-92-103 and ff., Strategic Highway Research Program, National Research Council, Washington, D.C., 1992.
- [2] Sagüés, A. and Powers, R., Corrosion, Vol. 52, p.508, 1996.
- [3] Bennett, J., Bartholomew, J., and Turk, T., "Cathodic Protection Criteria Related Studies Under SHRP Contract", Paper No. 323, Corrosion/93, NACE International, Houston, Texas, 1993.
- [4] Flis, J., Sabol, S., Pickering, H.W., Sehgal, A., Osseo-Asare, K., and Cady, P., Corrosion, Vol.49, p. 601, (1993).
- [5] Bartholomew, J. et al, Report SHRP-S-670, Strategic Highway Research Program, National Research Council, Washington, 1993.
- [6] Sagüés, A.A., and Powers, R.G., "Corrosion and Corrosion Control of Concrete Structures in Florida - What can be learned?" in Proceedings International Conference on Repair of Concrete Structures, pp.49-55, Svolvaer, Norway, 28-30 May, 1997.
- [7] Weyers, R.E., Prowell, B.D., Al-Qadi, I.L., Sprinkel, M.M., Vorster, M., "Concrete Bridge Protection, Repair, and Rehabilitation Relative to Reinforcement Corrosion: A Methods Application Manual", SHRP-S-360, Washington, DC:National Research Council, 1993.
- [8] Sagüés Alberto. A., Kranc, S.C., Francisco Presuel-Moreno, David Rey, Andres Torres-Acosta, Lan Yao, "Corrosion Forecasting For 75-Year Durability Design Of Reinforced Concrete", Final Report to FDOT, Contract BA-502, December 31, 2001.
- [9] Sagüés, A.A., Kranc, S.C., Al-Mansur, S. and Hierholzer, S., "Factors Controlling Corrosion of Steel-Reinforced Concrete Substructure in Seawater", Final Report to FDOT, W.P.I. No. 0510537, December 1994.
- [10] Al-Mansur, S., "Effect of Moisture Application on The Corrosion Behavior of Reinforcing Steel in Marine Bridge Substructures", MSc. Thesis, University of South Florida, Tampa, 1992.
- [11] Sagüés, A.A., "Electrochemical Impedance of Corrosion Macrocells on Reinforcing Steel in Concrete", Paper No. 132, Corrosion / 90, NACE International, Houston, 1990.

- [12] Sagüés, A.A., Perez-Duran, H.M., and Powers, R.G., "Corrosion Performance of Epoxy-Coated Reinforcing Steel in Marine Substructure Service", Corrosion Vol. 47, No. 11, p. 884, 1991.
- [13] Sagüés, A., "Corrosion Measurement Techniques for Steel in Concrete", Paper No. 353, 22 pp., Corrosion/93, National Assoc. of Corrosion Engineers, Houston, 1993.
- [14] Flis, J., Pickering H.W., and Osseo-Asare, K., Corrosion vol. 51, No. 8, p. 602, 1995.
- [15] Tia et al "Extension Study of Field and Laboratory Study of Modulus of Rupture and Permeability of Structural Concrete in Florida for Development of a Concrete Performance Specification", Final Report to Florida D.O.T., WPI 0510384, Report FL/DOT/RMC/0384-3366, December, 1993.
- [16] Babei, K., Purvis, R., Clear, K. and Weyers, R., "Participant's Workbook for Workshop of SHRP Research Projects related to Methodology for Concrete Removal, Protection and Rehabilitation", Wilbur Smith Associates, Falls Church, VA, June 1996.
- [17] Sagüés, A.A., Scannel, W. and Soh, F.W., "Development of a Deterioration Model to Project Future Concrete Reinforcement Corrosion in a Dual Marine Bridge", in Proc. International Conference on Corrosion and Rehabilitation of Reinforced Concrete Structures, Orlando, FL, Dec. 7-11, 1998, CD ROM Publication No. FHWA-SA-99-014, Federal Highway Administration, 1998.
- [18] Tuutti, K., "Corrosion of Steel in Concrete" (ISSN 0346-6906), Swedish Cement and Concrete Research Institute, Stockholm, 1982.
- [19] Torres-Acosta, A.A., and Sagüés, A.A., "Concrete Cover Cracking with Localized Corrosion of the Reinforcing Steel", p. 591 in Proc. of the Fifth CANMET/ACI Int. Conf. on Durability of Concrete, SP-192, V.M Malhotra, Ed., American Concrete Institute, Farmington Hills, Mich., U.S.A., 2000.
- [20] Scannel, W., Soh, F., Sohanghpurwala, A. A., and Sagüés, A., "Assessment of Rehabilitation Alternatives for Bridge Substructure Components" Final Report, CONCORR, Inc., Ashburn, VA, 1998.
- [21] Andrade, C. and Alonso, C., "Values of Corrosion Rate of Steel in Concrete in Order to Predict Service Life of Concrete Structures", in "Application of Accelerated Corrosion Tests to Service Life Prediction of Materials", STP 1194, G. Cragolino, Ed., ASTM, Philadelphia, 1992.
- [22] Li, L. and Sagüés, A.A., Corrosion, Vol. 57, pp.19-28, 2001.

- [23] Bamforth, P., "Improving the Durability of Concrete by the Use of Mineral Additives", Paper presented at "Concrete Durability in the Arabian Gulf", Bahrain Society of Engineers, 19-21, March 1995.
- [24] Sagüés, A.A., Powers, R.G., and Kessler, R., "Corrosion Performance of Epoxy-Coated Rebar in Florida Keys Bridges", Paper 06142, 13 pp., Corrosion/2001, NACE International, Houston, TX, 2001.
- [25] Sagüés, A.A., "Corrosion of Epoxy-Coated Rebar in Florida Bridges", Final Report to Florida D.O.T., WPI No. 0510603, May, 1994, available from Florida Department of Transportation, Research Center, Tallahassee, Florida.
- [26] Kessler, R. and Powers, R. Interim Report, Corrosion Evaluation of Substructure, Long Key Bridge, Corrosion Report No. 87-9A, Materials Office, Florida Department of Transportation, Gainesville, 1987.
- [27] Sagüés, A., Powers, R. and Kessler, R., "Corrosion Processes and Field Performance of Epoxy-Coated Reinforcing Steel in Marine Substructures", Paper No. 299, Corrosion/94, NACE International, Houston, 1994.
- [28] Kessler, R. and Powers, R., "Zinc Metallizing for Galvanic Cathodic Protection of Steel reinforced Concrete in a Marine Environment", Paper No. 324, Corrosion/90, NACE International, Houston, 1990.
- [29] Sagüés, A., Powers, R., Zayed, A., "Marine Environment Corrosion of Epoxy-Coated Reinforcing Steel", in Corrosion of Reinforcement in Concrete, C. Page, Treadaway, K., and Bamforth, P., Eds., pp.539-549, Elsevier Appl. Sci., London-New York, 1990.
- [30] Sagüés, A., and Powers, R., "Effect of Concrete Environment on the Corrosion Performance of Epoxy-Coated Reinforcing Steel", Paper No. 311, Corrosion/90, NACE International, Houston, 1990.
- [31] Sagüés, A. and Powers, R. "Coating Disbondment in Epoxy-Coated Reinforcing Steel in Concrete - Field Observations", Paper No. 325, Corrosion/96, NACE International, Houston, 1996.
- [32] Hartt, W., Lee, S.K., and Costa, J., "Condition Assessment and Deterioration Rate Projection for Chloride Contaminated Concrete Structures" p.82 in Repair and Rehabilitation of Reinforced Concrete Structures: The State of the Art, Silva-Araya, W.P., de Rincon, O. T., and Pumarada O'Neill, L., Eds., ASCE, Reston, VA, 1998.
- [33] Berke, N.S., and Hicks, M.C., "Estimating the Life Cycle of Reinforced Concrete Decks and Marine Piles using Laboratory Diffusion and Corrosion Data", p. 207

- in Corrosion Forms and Control for Infrastructure, ASTM STP 1137, Victor Chaker, Ed., ASTM, Philadelphia, 1992.
- [34] Andrade, C., Alonso, C. and Goni, S., "Possibilities for Electrical Resistivity to Universally Characterized Mass Transport Processes in Concrete", p.1639, in Concrete 2000, Vol. 2., R.K. Dhir, and M.R. Jones, Eds., E. & F.N. Spon, London, 1993.
- [35] Clear, K.C., "Effectiveness of Epoxy-Coated Reinforcing Steel", Concrete International, p. 58, Vol. 14, May 1992.
- [36] McDonald, D.B, Pfeifer, D.W. and Sherman, M.R, "Corrosion Evaluation of Epoxy-Coated, Metallic-Clad and Solid Metallic Reinforcing Bars in Concrete", Report No. FHWA-RD-98-153, Nat. Tech. Info. Service, Springfield, VA, 1998.
- [37] Sagüés, A.A. and Kranc, S.C. "Model for a Quantitative Corrosion Damage Function for Reinforced Concrete Marine Substructure" in Rehabilitation of Corrosion Damaged Infrastructure, p.268, Proceedings, Symposium 3, 3rd. NACE Latin-American Region Corrosion Congress, P.Castro, O.Troconis and C. Andrade, Eds., ISBN 970-92095-0-7, NACE International, Houston, 1998.
- [38] Cady, P.D., and Weyers, R.E., "Deterioration Rules of Concrete Bridge Decks", Journal of Transportation Engineering, American Society of Civil Engineers, Vol. 110, No. 1, January 1984, pp. 35 - 44.
- [39] Weyers, R., "Corrosion Service Life Model Concrete Structures", p.105, in Repair and Rehabilitation of Reinforced Concrete Structures: The State of the Art, Silva-Araya, W.P., de Rincon, O. T., and Pumarada O'Neill, L., eds, ASCE, Reston, VA, 1998.
- [40] Thomas, M.D.A. and Bentz, E.C. "Life 365 - Computer Program For Predicting The Service Life And Life-Cycle Costs Of Reinforced Concrete Exposed To Chlorides", distributed by The Concrete Corrosion Inhibitors Association, 2000.
- [41] Mangat, P., and Molloy, B., "Prediction of long term chloride concentration in concrete", Materials and Structures, Vol. 27, p.338-346, 1994.
- [42] Nilsson, L.O., Massat, M., and Tang, L., "The Effect of Non-linear Chloride Binding on the Prediction of Chloride Penetration into Concrete Structures", p. 469 in Durability of Concrete, ACI Publication SP-145, Malhotra, V.M., Ed., American Concrete Institute, Detroit, 1994.
- [43] Sagüés, A., and Kranc, S.C., "Effect of Structural Shape and Chloride Binding on Time to Corrosion of Steel in Concrete in Marine Service", p. 105-114 in Corrosion of Reinforcement in Concrete Construction, C.L. Page, Bamforth, P.B., and Figg, J.W., Eds, The Royal Society of Chemistry, Cambridge, 1996.

- [44] Dühr, R., Jones, M., Byars, E., and Shaaban, I., "Predicting concrete durability from its absorption", p. 1177, in "Durability of Concrete", Malhotra, V., Ed., SP 145, ACI, Detroit, 1994.
- [45] Bertolini, L., Bolzoni, F., Pastore T., and Pedferri, P., "New Experiences on Cathodic Prevention of Reinforced Concrete Structures", pp. 390-398 in "Corrosion of Reinforcement in Concrete Construction", C. Page, Bamforth, P., and Figg, J., Eds. Society for Chemical Industry, Special Publication, No. 183, London, 1996.
- [46] Sagüés, A. A., Kranc S.C., and Presuel-Moreno, F.J., "Applied Modeling for Corrosion Protection Design for Marine Bridge Substructures", Report No. 0510718, June, 1997, available from Florida Department of Transportation, Research Center, Tallahassee, Florida.
- [47] Presuel-Moreno, F.J., Sagüés, A. A., and S.C. Kranc, "Steel Activation in Concrete Following Interruption of Long Term Cathodic Polarization", Paper #02259, Corrosion/2002, NACE International, Houston, 2002.

10. TABLES

Table 1 - Elevation Ranges and Elements for Escambia Bay Bridges

Piles	Number in water	Perimeter (m)	Range Height (m)			Range Area, Both Bridges (m ²)		
			T i=1	LS i=2	US+AS i=3	T i=1	LS i=2	US+AS i=3
0.91-m	1218	2.87	0.45	0.3	1.5	1573	1049	5243
1.37-m	268	4.31	0.45	0.3	1.5	520	347	1733
Both Piles (m ²):						2093	1395	6976
Number of Elements for Ae = 0.1 m ² , Both Piles (N _i)						20928	13952	69761

Table 2 -Escambia Bay Bridges Parameters

	TIDAL (i=1)	D(in ² /y)	Cs(%)	D(m ² /s)	Cs(kg/m ³)
T i=1	AVG:	1.04e-02	0.98	2.13e-13	25.02
	STDEV:	7.0e-03	0.47	1.4e-13	12.1
LS* i=2	AVG:	5.00e-03	0.60	1.0e-13	15.3
	STDEV	2.5e-03	0.30	5.1e-14	7.6
US+AS i=3	AVG:	2.42e-03	0.385	4.95e-14	9.80
	STDEV:	1.3e-03	0.20	2.6e-14	5.2

*assigned values

Table 3 - Positions Tested, Escambia Bay Bridges

Pile	Number or test spots	Strands				Stirrups			
		Avg (cm)	St. Dev. (cm)	Highest (cm)	Lowest (cm)	Avg (cm)	St. Dev. (cm)	Highest (cm)	Lowest (cm)
0.91-m	47	4.04	1.12	5.71	2.54	2.84	0.66	5.08	1.90
1.37-m	14	3.51	1.24	5.08	1.27	2.64	0.51	3.17	1.90

Table 4 – Florida Keys Bridges

BRIDGE	7 MILE (7MI)	NILES CHANNEL (NIL)	LONG KEY (LKY)	INDIAN KEY (INK)	CHANNEL #5 (CH5)
FDOT Bridge Number	900020	900117	900094	900095	900098
Year Built	1980	1982	1980	1981	1981
Number of Bents	264	38	102	19	35
ECR Source	Florida Steel	Bethlehem Steel	Florida Steel	Bethlehem Steel	Bethlehem Steel
Epoxy Coating Powder	Scotchkote 213	Scotchkote 213	Scotchkote 213 Hysol	Scotchkote 213	Scotchkote 213
Coating Applicator	Rezcom (Drilled Shafts) Santa Fe	Lane Metals MCP	Rezcom	MCP Lane Metals	MCP
Cement Type	II	II and III	I and II	II	III
Initial Concrete Cl ⁻ Content (kg/m ³)	1.7	0.15	0.15	0.65 - 2.1	0.15

Table 5 - Cumulative Spall Numbers Observed To Date Of Inspection, Florida Keys Bridges

BRIDGE	7 MILE (7MI)	NILES CHANNEL (NIL)	LONG KEY (LKY)	INDIAN KEY (INK)	CHANNEL #5 (CH5)
Year Built	1980	1982	1980	1981	1981
Number of Bents	264	38	102	19	35
INSPECTION DATE			CUMULATIVE NUMBER OF SPALLS		
1986			1		
1987			3		
1988	8	17	17		
1989	22				
1990	58	34	45	2	
1993 (1st)					2
1993 (2nd)	175	54	83	10	18
1995	204	67	90	16	
1996	232			16	37
1998	290	81	123	23	47
1999	324				
2000	452				58

Table 6 – Calculation Parameters, Florida Keys Bridges

Af	Surface area of bent exposed to severe corrosion	20 m ²
Ae	Typical spall area	0.3 m ²
C _T	ECR chloride concentration threshold	1.55 kg/m ³
Cs	Average surface chloride concentration	14 kg /m ³
s _{cs}	Standard deviation of surface chloride concentration	Cs/4
C _{smax}	Maximum surface chloride concentration	14 kg/m ³
x	Average rebar cover	76 mm
s _x	Standard deviation of rebar cover	x/4
D	Average apparent chloride diffusion coefficient	2 10 ⁻⁷ cm ² /sec
s _d	Standard deviation of app. diff. coeff.	D/4
k'	Proportionality constant for propagation time (Percentages indicate fraction of the surface assigned to the value).	0.14 y/mm (2%); 0.28 y/mm (4%); 0.56 y/mm (8%).

Note: Cs, x and D were assumed to be distributed as in a standard distribution, but truncated by zero and as shown by C_{smax}, and normalized accordingly.

11. FIGURES

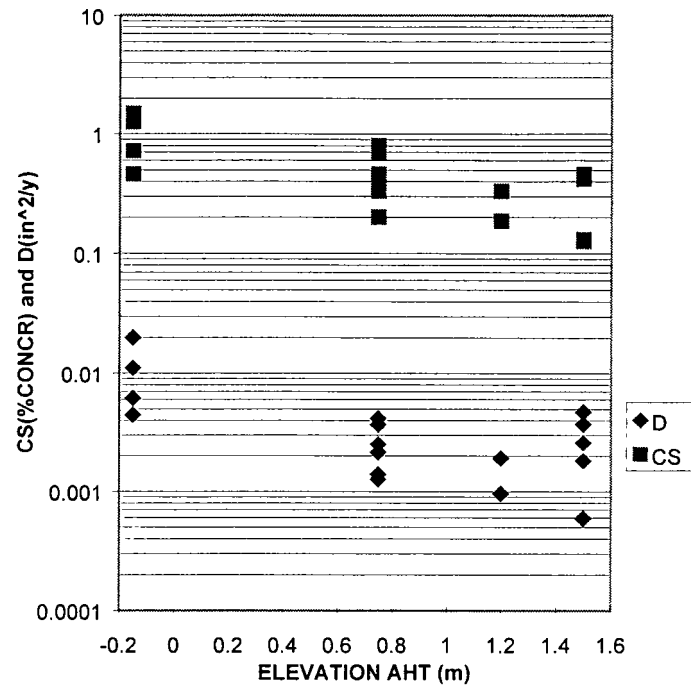


Figure 1. D and Cs as a function of elevation [17]

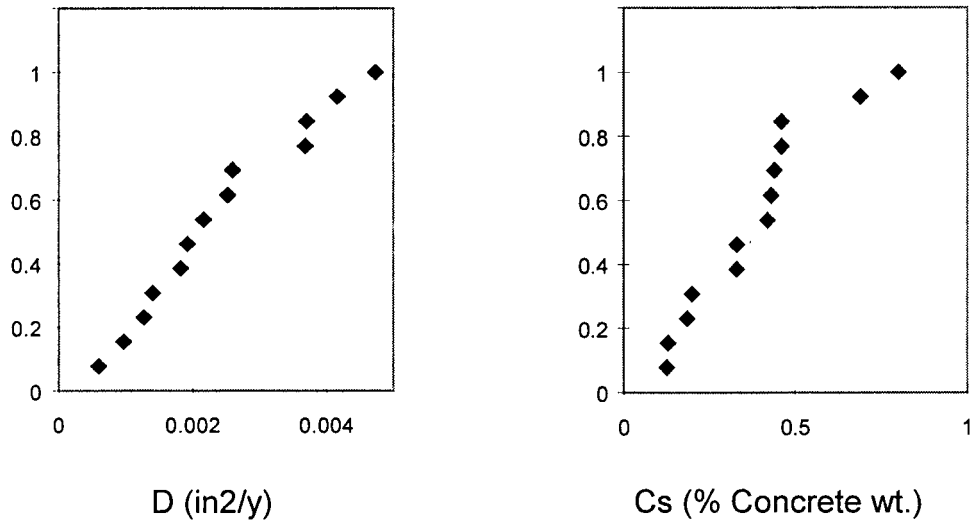


Figure 2. Cumulative normal distributions (dashed lines) based on the average and standard deviation values in Table 2 for D and C_s in elevation ranges 2 and 3, and actual distribution of values [17].

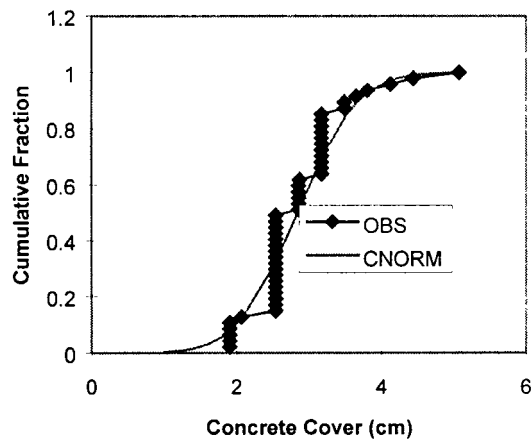


Figure 3. Cumulative normal distribution of stirrup concrete cover and observed values (OBS) for the 0.91-m (3-ft) piles [17].

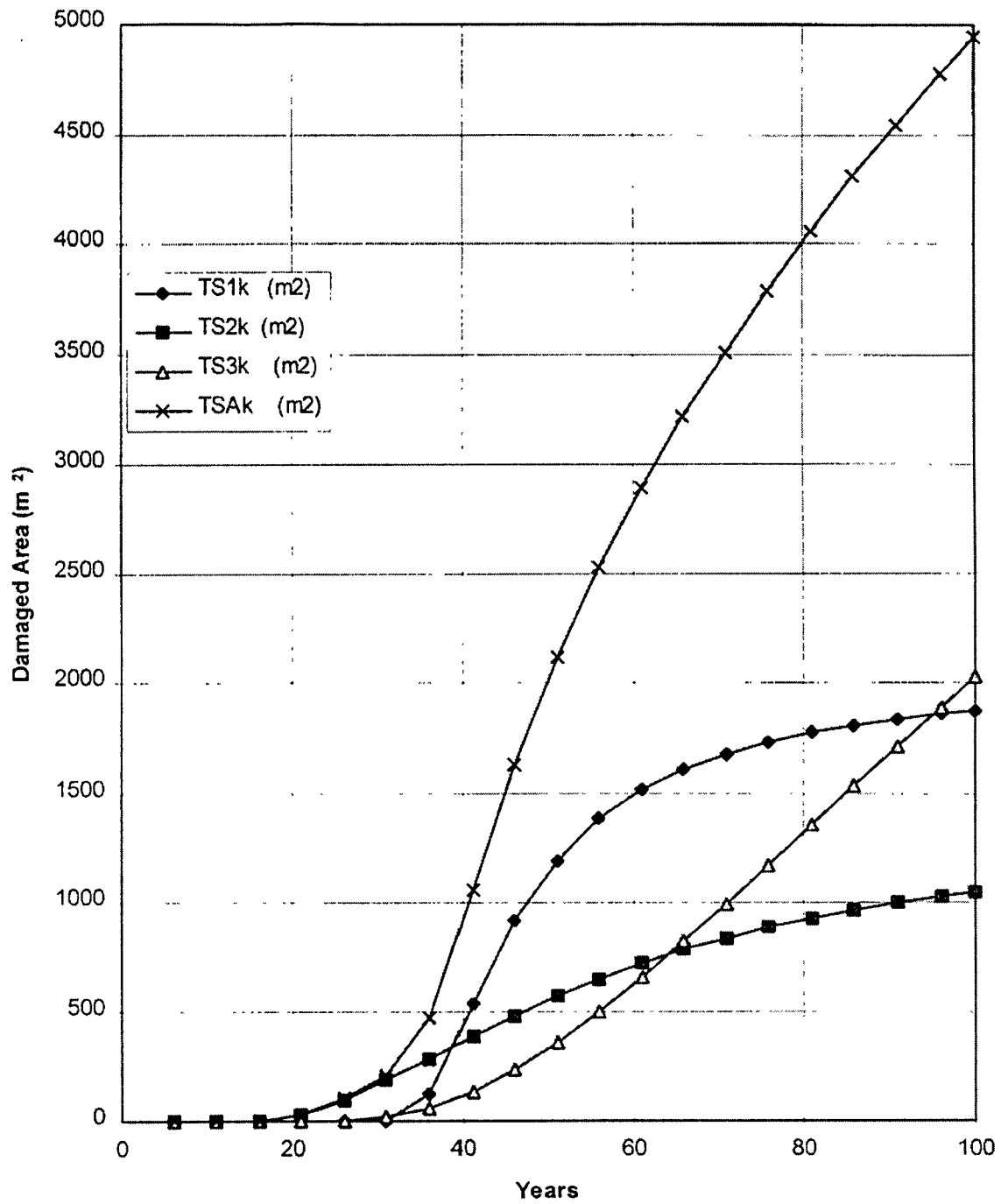


Figure 4. Deterioration model output for Case A ($C_T = 1.6 \text{ kg/m}^3$) [17].

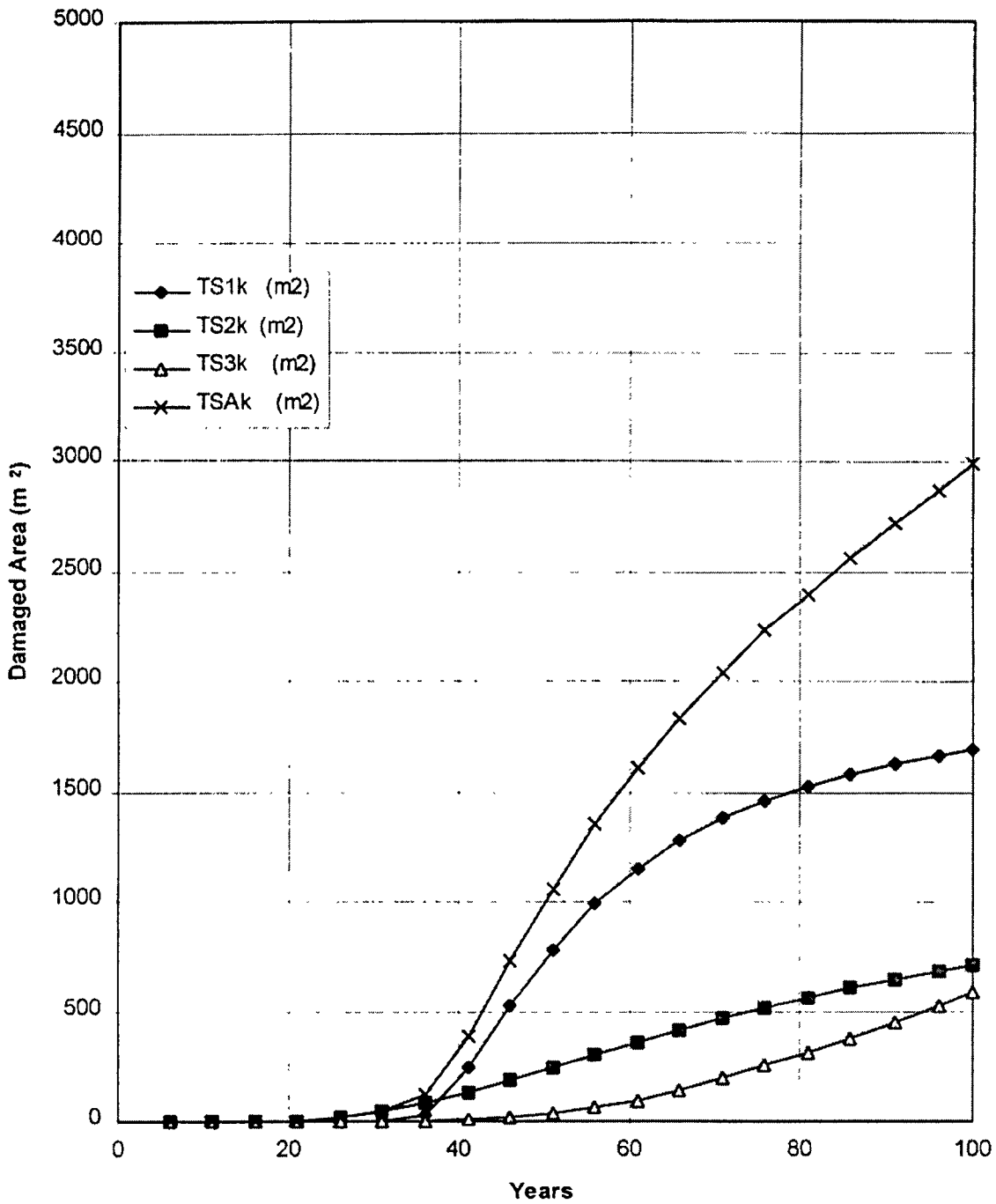


Figure 5. Deterioration model output for Case B ($C_T = 3.2 \text{ kg/m}^3$) [17].

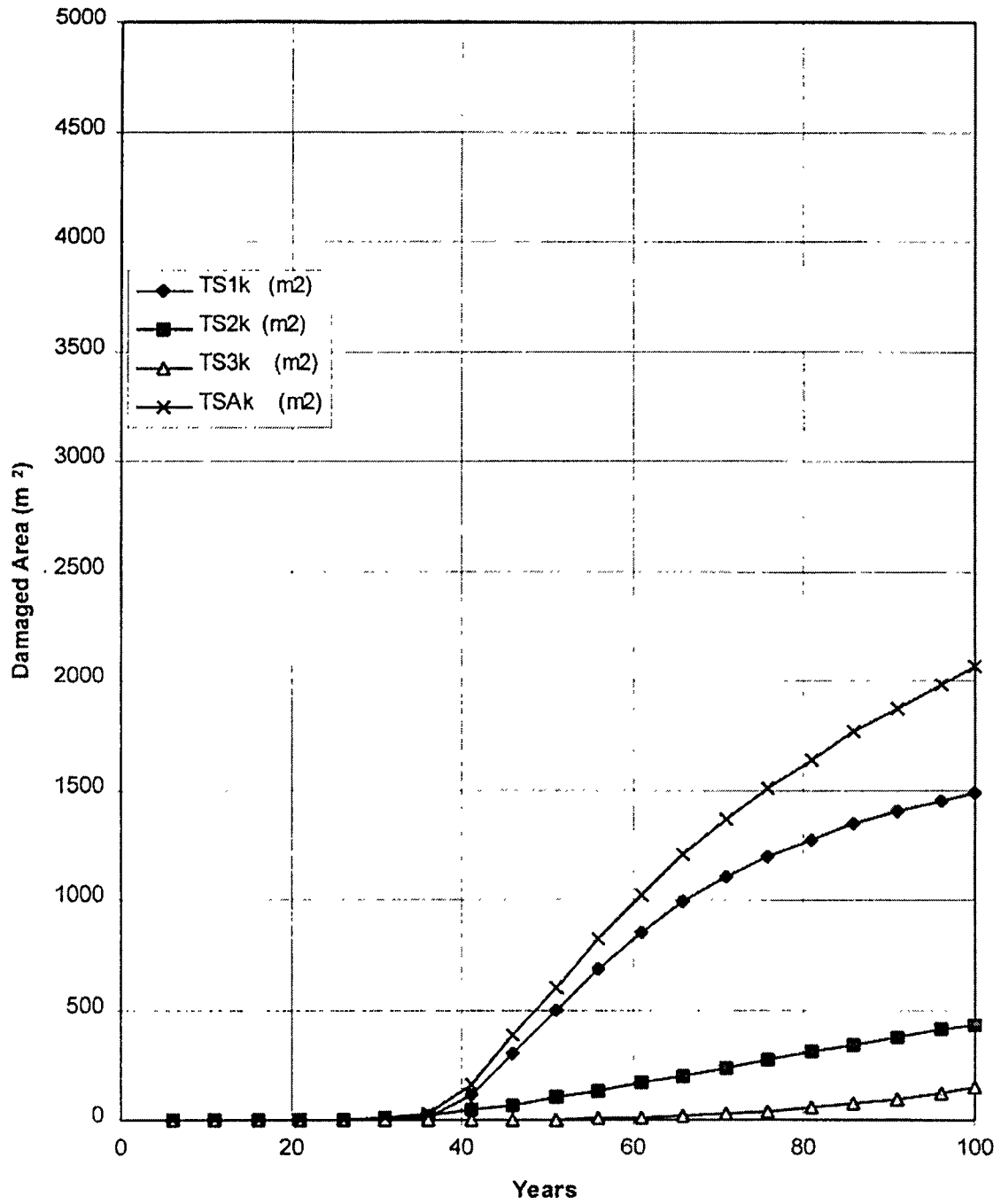


Figure 6. Deterioration model output for Case C ($C_T = 4.8 \text{ kg/m}^3$) [17].

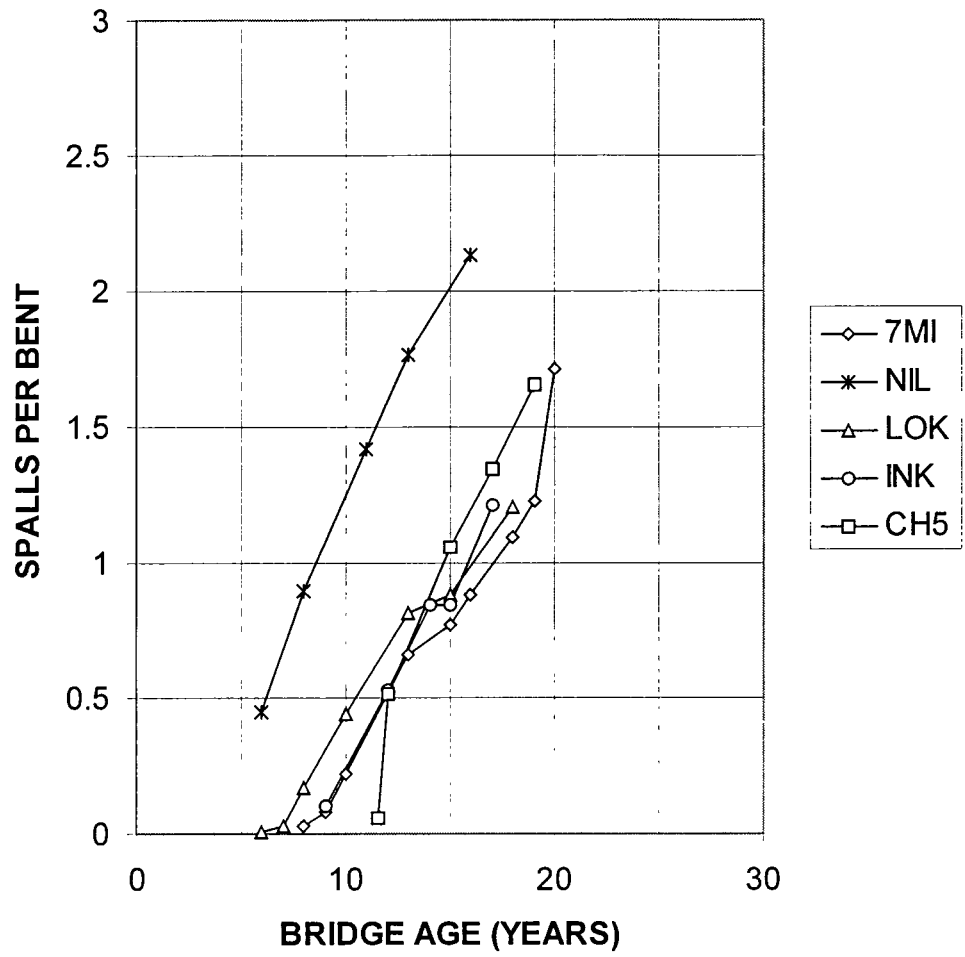


Figure 7. Progress n of corrosion as function of time. Data from Table 5 were normalized by dividing by the number of bents in each bridge [24].

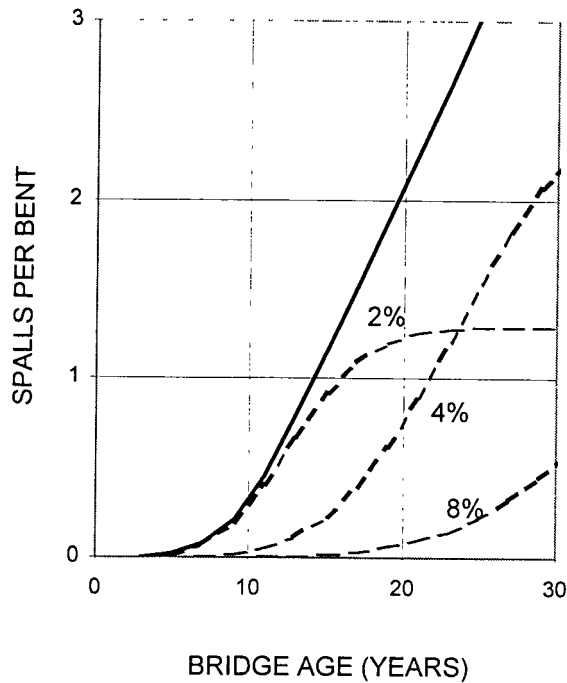


Figure 8 - Illustration of a projected damage function generally replicating the features and values of the behavior in Figure 7. The solid line corresponds to the total damage projection. The dashed lines correspond to the partial damage from each of the rebar assembly fractions considered: 2% of the rebar with $k=0.14$ y/mm; 4% with $k=0.28$ y/mm and 8% with $k=0.56$ y/mm. Adding up the partial damages yields the total damage [24].

12. UNIT CONVERSIONS TABLE

CONVERSION FACTORS, US CUSTOMARY TO METRIC UNITS

<i>Multiply</i>	<i>by</i>	<i>to obtain</i>
inch	25.4	mm
foot	0.3048	meter
square inches	645	square mm
cubic yard	0.765	cubic meter
pound/cubic yard	0.593	kg/cubic meter
inch ² /year	2.046 10 ⁻⁷	cm ² /sec
gallon/cubic yard	4.95	liter/cubic meter
standard cubic feet/hour	466.67	ml/minute
ounces	28.35	gram
pound	0.454	kilogram
pound (lb)	4.448	newtons
kip (1000 lb)	4.448	kilo newton (kN)
pound/in ²	0.0069	MPa
kip/in ²	6.895	MPa
ft-kip	1.356	kN-m
in-kip	0.113	kN-m

